Materials Science and Engineering A 528 (2011) 6203–6209

Contents lists available at ScienceDirect

Materials Science and Engineering A

journal homepage: www.elsevier.com/locate/msea

Thermo mechanical properties and plastic deformation of gold nanolines and gold thin films

Sven Olliges[a], Stephan Frank[a], Patric A. Gruber[b], Vaida Auzelyte[c], Harun Solak[c], Ralph Spolenak[a,*]

[a] ETH Zurich, Department of Materials, Laboratory for Nanometallurgy, Wolfgang-Pauli-Strasse 10, CH-8093 Zurich, Switzerland
[b] Karlsruhe Institute of Technology (KIT), Institute for Applied Materials (IAM), Postfach 3640, D-76021 Karlsruhe, Germany
[c] Paul-Scherrer-Institute, Laboratory for Micro- and Nanotechnology, CH-5232 Villigen, Switzerland

ARTICLE INFO

Article history:
Received 2 February 2011
Received in revised form 13 April 2011
Accepted 14 April 2011
Available online 21 April 2011

Keywords:
Gold nanolines
Gold thin films
Yield strength
Diffusion creep
Temperature

ABSTRACT

The material behavior of nano-shaped and -scaled materials is a key issue for their system integration in modern micro electro-mechanical systems (MEMS). In this article, the thermo mechanical properties of (i) homogeneous gold thin films with a thickness of 20 nm on polyimide substrate and (ii) gold nanoline ensembles with 40 nm width, 20 nm height and 1 mm length on polyimide substrate were measured using the synchrotron based $\sin^2(\varphi)$-tensile testing technique. Both, passivated and unpassivated samples were tested in a temperature range of 173–393 K. As main findings: (i) homogeneous thin films are remarkably stronger than the nanolines, (ii) the yield strength shows a strong temperature dependence, and (iii) the yield strength of passivated samples is significantly increased compared to their unpassivated counterparts. The activation energy also shows a pronounced temperature dependency and indicates plastic deformation controlled by (i) dislocation motion for temperatures below 223 K, (ii) diffusion along (1 1 1) surfaces in the temperature range of 223–343 K and (iii) diffusion along the remaining surfaces (others than (1 1 1)) in the temperature range of 334–393 K.

1. Introduction

Material properties can be classified as either *intrinsic* properties such as the Young's modulus E, the shear modulus μ or the Poisson's ratio ν or *extrinsic* properties like the hardness H and the yield strength σ_y. While the *intrinsic* properties are "ideal" properties derived from physical fundamentals, the *extrinsic* properties are strongly affected by the microstructure and can be varied over two orders of magnitude by grain refinement (Hall-Petch effect), work hardening (Taylor effect), solid solution, precipitates and dispersoids [1]. All these hardening effects comprise dislocation motion and their mutual interaction and usually show increasing mechanical strength when (additional) constraints such as reduction of external dimensions, grain refinement, increased dislocation density, etc. are introduced into the microstructure (size effect). However, this approach reaches a limit of validity for very strong constraints such as in nano-crystalline materials and nano-structures. E.g., when the grains become too small for the formation of a dislocation loop, the Hall-Petch relation is no longer valid and a decrease in yield strength for grain sizes smaller than about 10–15 nm (theoretical value) is found [2–6]. Therefore, the mechanical properties of nano-structures with external dimensions of this size range might be controlled by diffusion instead of dislocation based mechanisms. This might even lead to strong temperature dependent mechanical properties and strain rate effects, which are not observed for macroscopic fcc structures below homologous temperatures of 0.5 [7].

Indeed, thickness/dimension and temperature dependent yield strength has been observed for as deposited homogeneous gold thin films with thicknesses in the range of 80–500 nm on Kapton™ substrate, where the yield strength varies (i) for 80 nm thick gold thin films with mean grain sizes of about 125 nm between 700 MPa (123 K) and 100 MPa (423 K) and (ii) for measurements at RT between 450 MPa (80 nm – mean grain size of 125 nm) and 300 MPa (500 nm – mean grain size of 295 nm) [8]. It was also shown, that passivation of the 80 nm gold thin films by SiN_x raises the yield strength from 450 MPa to 900 MPa for testing at RT. Similar effect of passivation (oxide layer) on the mechanical properties was observed also for Cu thin films on Si substrate, which were tested in ambient and vacuum environment [9]. Freestanding polycrystalline gold thin films with thicknesses of about 125 nm and mean grain sizes of about 60 nm were found to show relaxation even at RT [10]. Single crystalline gold pillars with diameters in the micron/submicron range (prepared by focused ion beam (FIB) milling) were investigated by uniaxial compression using nanoindentation system [11]. The yield strength of these pillars follows

* Corresponding author at: Laboratory for Nanometallurgy (LNM), Department of Materials, ETH Hönggerberg, Wolfgang-Pauli-Strasse 10, CH-8093 Zurich, Switzerland. Tel.: +41 44 632 2590; fax: +41 44 632 1101.
E-mail address: ralph.spolenak@mat.ethz.ch (R. Spolenak).

0921-5093/$ – see front matter © 2011 Elsevier B.V. All rights reserved.
doi:10.1016/j.msea.2011.04.041

a power law $\sigma_y \sim d^{-0.61}$ and the highest yield strength of about 560 MPa was obtained for pillars with 180 nm diameter (smallest diameter tested in this study). Bending tests of polycrystalline gold nanowires with diameters of 250 nm and 40 nm show yield stresses of 3.5 GPa and 5.6 GPa, respectively [12]. The bonding strength of atomic gold chains was measured by pushing gold coated AFM/STM tips into a gold substrate followed by retracting the tip and necking of the contact [13–15]. The bonding force was measured to be around 1.5 nN, which gives together with an assumed atomic radius of 135 pm a yields strength of up to 25 GPa. The necking of the nano-contact to an atomic chain is supported by MD simulations [16]. Larger gold nanowires with a square base of 4 nm × 4 nm and a length of 12 nm were investigated by atomistic simulations [17]. The yield strengths along the [1 1 1] and [1 0 0] directions were found to be 4 GPa but the strain to fracture was found to be approximately 2.5 times larger for the [1 1 0] direction compared to the [1 1 1] direction, which is due to the differences in Young's modulus. For the [1 0 0] direction also a strong asymmetry in tensile and compressive yield strength is obtained. For even smaller gold nanowires with [1 0 0] orientation and a square base of 1.83 nm × 1.83 nm, a surface tension induced phase transformation from fcc to bct lattice system is reported [18]. Another increasingly relevant effect in small dimensions below 10 μm is the appearance of geometrically necessary dislocations (GND) [19,20]. Their influence is of particular importance if bending moments are involved such as in bending testing and nanoindentation.

The present manuscript investigates the thermo mechanical properties of (i) homogeneous gold thin films with a thickness of 20 nm and (ii) gold nanolines with dimensions of 40 nm width, 20 nm height and 1 mm length. Both types of samples were deposited on 125 micron Kapton™ foil (polyimide) by top-up approaches and tensile tested in passivated as well as unpassivated state using the synchrotron based $\sin^2(\varphi)$-tensile testing technique [21].

2. Experimental

Gold nanolines were produced on 125 μm thick Kapton™ (polyimide) foil by extreme-ultra-violet interference lithography (EUV-IL) using the corresponding beamline at the Swiss Light Source (SLS) of the Paul Scherrer Institute in Villigen, Switzerland [22,23]. Patterns of parallel nanolines with a periodicity of 100 nm, about 40 nm width and 1 mm length were produced by exposure of PMMA/HSQ double layer photo resist by EUV interference patterns followed by etching of the photo resist layer. Subsequently, the line patterns were metalized to about 20 nm height by thermal evaporation of gold. In order to improve the adhesion of the gold lines on the Kapton™ substrate, a 2 nm Cr interlayer was applied. The final arrangement consists of an ensemble of about 5000 parallel and identical nanolines with the "external dimensions" of 0.5 mm × 1 mm, whereas each nanoline has a cross section of about 40 nm × 20 nm and a length of 1 mm. Details of the nanoline sample fabrication are reported in [22]. A SEM snapshot of the nanolines is shown in the inset of Fig. 2. Homogeneous gold thin films having a similar thickness of 20 nm were produced by thermal evaporation of gold on Kapton™ substrate, which was again pre-coated with 2 nm Cr for an improved adhesion. The deposition parameters are the same for both samples types and resulted in a mean grain size of 20–30 nm. The gold nanolines as well as the homogeneous thin films showed a (1 1 1) out-of-plane texture as expected for fcc thin film systems (cf. Fig. 8 in [24]).

Parts of the samples were passivated by the deposition of about 700 nm parylene on top of the gold nanolines and thin films. In order to improve the adhesion of the parylene on the gold, again a 2 nm Cr adhesive interlayer was applied.

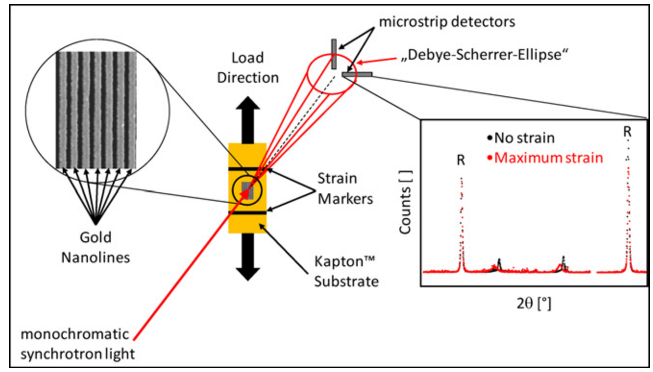

Fig. 1. Scheme of the experimental $\sin^2(\varphi)$-setup at the synchrotron. The "*R*" stands for the reference peaks (W powder in vacuum grease), which are non-strain sensitive.

The gold nanoline ensembles and thin films were tested at the Materials Science beamline at the Swiss Light Source (SLS) [25] using the $\sin^2(\varphi)$-tensile testing technique [21]. The samples were mounted in a tensile tester (Kammrath and Weiss) and placed at normal incidence in the X-ray beam with an energy of E = 7.97 keV. The energy of the X-rays was adjusted according to (i) normal beam incidence, (ii) the theoretical distance of the (1 1 1) planes at an angle of 70.54° with respect to the (1 1 1) out-of-plane texture and (iii) constructive interference according to Bragg's law in order to obtain a Debye-Scherrer ring (for detailed information see [21]). Unidirectional external stress is applied to the samples via stress transfer by loading the Kapton™ substrate with the tensile tester which results in extension and contraction of the gold lattice along the loading and transverse direction, respectively (please notice that the nanolines need to be aligned parallel to the loading direction of the tensile tester since particularly no stress is transferred in transverse direction [26]). The consequential elliptic distortion of the Debye-Scherrer ring is measured in terms of lattice strains using 2 linear single photon counting (second generation) microstrip detectors [27,28] mounted according to the principal axes of the ellipse. The lattice strains are converted into stresses using elasticity theory. The global strain applied by the tensile tester was measured by a set of strain markers in combination with an optical camera system (NIKON D80, 200 mm macro lens). Both, the optical images as well as the X-ray spectra were analyzed by homemade MatLab programs [29,30]. Please notice, that the $\sin^2(\varphi)$-technique provides relative stress values and the initial residual stress must be known in order to obtain absolute stress values [21]. Parts of the samples were tensile tested at different temperatures in the range of 173–393 K using a CryoJet (Oxford Instruments). Please notice that the sample temperature was cross-checked during setting up of the experiment with a thermocouple but not monitored during tensile testing in order to avoid any scratching and bending moment by the thermocouple. A scheme of the experimental setup is shown in Fig. 1.

3. Results

Typical relative stress–strain behavior is exemplarily discussed for gold nanolines in Fig. 2. Starting at the origin of the stress–strain diagram the stress initially follows a linear elastic behavior followed by a continuous transition to an upper plateau value σ_u at moderate loading. The upper plateau stress is kept even for higher loadings of up to 10% strain. Unloading the sample results in a linear stress relief followed by a continuous transition to a lower plateau σ_l, which is kept even for further unloading. The tensile test is finished when the Kapton™ substrate starts to buckle. Tables 1 and 2 give an overview on the tested samples (thickness/dimensions, pas-